Molecular Microbiology (2015) ■ doi:10.1111/mmi.13090

Association of UBP1 to ribonucleoprotein complexes is regulated by interaction with the trypanosome ortholog of the human multifunctional P32 protein

Alejandro Cassola,* María Albertina Romaniuk, Debora Primrose, Gabriela Cervini, Iván D'Orso† and Alberto Carlos Frasch
Instituto de Investigaciones Biotecnológicas-Instituto Tecnológico de Chascomús, UNSAM-CONICET, Buenos Aires, Argentina.

Summary

Regulation of gene expression in trypanosomatid parasitic protozoa is mainly achieved posttranscriptionally. RNA-binding proteins (RBPs) associate to 3′ untranslated regions in mRNAs through dedicated domains such as the RNA recognition motif (RRM). *Trypanosoma cruzi* UBP1 (TcUBP1) is an RRM-type RBP involved in stabilization/degradation of mRNAs. TcUBP1 uses its RRM to associate with cytoplasmic mRNA and to mRNA granules under starvation stress. Here, we show that under starvation stress, TcUBP1 is tightly associated with condensed cytoplasmic mRNA granules. Conversely, under high nutrient/low density-growing conditions, TcUBP1 ribonucleoprotein (RNP) complexes are lax and permeable to mRNA degradation and disassembly. After dissociating from mRNA, TcUBP1 can be phosphorylated only in unstressed parasites. We have identified TcP22, the ortholog of mammalian P32/C1QBP, as an interactor of TcUBP1 RRM. Overexpression of TcP22 decreased the number of TcUBP1 granules in starved parasites *in vivo*. Endogenous TcUBP1 RNP complexes could be dissociated *in vitro* by addition of recombinant TcP22, a condition stimulating TcUBP1 phosphorylation. Biochemical and *in silico* analysis revealed that TcP22 interacts with the RNA-binding surface of TcUBP1 RRM. We propose a model for the decondensation of TcUBP1 RNP complexes in *T. cruzi* through direct interaction with TcP22 and phosphorylation.

Accepted 9 June, 2015. *For correspondence. E-mail acassola@iibintech.com.ar; Tel. +54-11-4006-1500; Fax +54 11 4006-1559. †Present address: Department of Microbiology, University of Texas Southwestern Medical Center, 5323 Harry Hines Boulevard, Dallas, TX 75390-9048, USA.

Introduction

A controlled regulation of gene expression is required in every cell type in order to achieve homeostasis. This regulation can be exerted at different points, such as transcription initiation, elongation, mRNA processing, cytoplasmic export, translational efficiency and degradation (Moore, 2005). However, these mechanisms are not identical in mammalian and in trypanosomes, protozoan parasites of medical importance in the developing world (McCall and McKerrow, 2014). *Trypanosoma cruzi* is responsible for Chagas disease in the Americas, whereas *T. brucei* produces sleeping sickness in sub-Saharan Africa. These parasites use polycistronic transcription and co-ordinated trans-splicing and polyadenylation events to obtain mature messenger RNA (mRNA) molecules (Moretti and Schenkman, 2013). As a result, mRNAs coding for proteins unrelated in function are synthesized, on which translation efficiency and regulated decay dictate the final protein levels for every parasite stage (Clayton, 2013). The relevance of this regulation has an impact on the different life forms these parasites develop within their insect and vertebrate hosts, facing dissimilar immune systems and stress situations. Hence, in trypanosomes mRNA translation/decay is highly dependent on the RNA-binding proteins (RBPs) that associate with mRNAs, especially to the 3′ untranslated region (UTR) (Kolev *et al.*, 2014).

RBPs association to target transcripts is dependent on RNA-binding domains (RBDs), such as the RNA-recognition motif (RRM), one of the most characterized RBD in mammalian and trypanosome cells (De Gaudenzi *et al.*, 2005; Daubner *et al.*, 2013). This domain is typically composed by 90 amino acids, which adopts a $\beta_1\alpha_1\beta_2\beta_3\alpha_2\beta_4$ topology leading to the formation of an antiparallel β-sheet packed against two α-helices (Stefl *et al.*, 2005). The central β3 and β1 strands of the domain contain the RNP1 and RNP2 sequences respectively. These motifs expose three conserved aromatic residues on the surface of the β-sheet, forming the primary RNA-binding surface (Clery *et al.*, 2008).

Other domains accompanying RRMs in RBPs can provide a scaffold for protein interactions and additional

regulation (Lunde *et al.*, 2007). This is the case of low complexity (LC) sequences, defined by the presence of repetitive amino acids. LC sequences enriched in RBPs and mRNA metabolism related proteins resemble prion-like domains, allowing these proteins to form physiological and microscopically visible mRNA granules. However, in different neuronal pathologies, these domains can form self-propagating amyloids of ribonucleoprotein (RNP) aggregates, leading to toxicity due to perturbations of normal posttranscriptional control (Ramaswami *et al.*, 2013). Thus, the dynamic association of different RBPs in RNP complexes seems to regulate the assembly of RNA granules (Kato *et al.*, 2012).

We have previously described and characterized the presence of starvation induced mRNA granules (mRNA granules hereafter) in trypanosomes (Cassola *et al.*, 2007). Although different RNA granules have been described in a wide variety of protozoa (Kramer, 2014), there is no mechanistic description of their formation or assembly. In trypanosomes, many types of RNP granules can be detected, whereas others are formed under stress conditions, albeit only P bodies seem to be present constitutively (Cassola, 2011; Kramer, 2014). Of these, mRNA granules seem to have a relevant role during low nutrient availability in the insect vector, allowing the protection of transcripts from degradation in a translational quiescent state. Soon after nutrients are available, protected mRNAs can reenter translation, showing the reversibility of these non-membranous structures (Cassola, 2011). One of the first proteins to be detected and characterized for its association to mRNA granules was TcUBP1 from *T. cruzi* (Cassola *et al.*, 2007). TcUBP1 has a single RRM with the characteristic βαββαβ fold and an additional hairpin (β4-β5) in the β-sheet, resulting in an enlarged RNA-binding surface (Volpon *et al.*, 2005). A Gly-rich domain downstream the RRM allows TcUBP1 homodimerization (D'Orso and Frasch, 2002). Additional protein–protein interactions might involve the accessory N and C-terminal LC sequences, each composed by 40% and 50% Gln respectively (D'Orso and Frasch, 2001). TcUBP1 associates with mRNA granules through the RRM, as deletions of this domain and point mutations in the RNP1 motif abrogate association with these structures (Cassola *et al.*, 2007; Cassola and Frasch, 2009). Under normal conditions TcUBP1 interacts with structural motifs found in the 3′ UTR of functionally related transcripts in the cytoplasm, suggesting co-ordinated regulation of these transcripts in posttranscriptional operons (Noe *et al.*, 2008). Thus, collected biophysical information from TcUBP1 makes this protein a model RBP in trypanosomes (D'Orso and Frasch, 2002; Volpon *et al.*, 2005; Cassola *et al.*, 2007; 2010; Cassola and Frasch, 2009). Although RRM-type RBPs have been studied in trypanosomes for more than a decade, detailed information on the regulated function of these proteins is lacking. This observation raises the question on whether there are other players compromising the association of RBPs with RNA in kinetoplastid parasites.

Here, we explored the behavior of TcUBP1 as a component of condensed and lax RNP complexes. While analyzing the possible association of regulatory proteins with the RRM of TcUBP1, we found a strong association with TcP22, the *T. cruzi* ortholog of human P32/C1QBP, a multifunctional protein. The relevance of the TcUBP1-TcP22 interaction was analyzed in the context of starvation-induced TcUBP1 granules *in vivo* and in the disassembly of normal TcUBP1 RNP complexes *in vitro*. Our results led us to propose a model for the dynamic decondensation of TcUBP1 RNP complexes in *T. cruzi*.

Results

Growth conditions modulate the condensation of RNP complexes containing TcUBP1 and its modification

Using localization approaches we have previously gained valuable information on the function and dynamics of different proteins related to mRNA metabolism in *T. cruzi*. Under conditions of starvation TcUBP1 colocalizes completely with poly(A) mRNA in mRNA granules (Fig. 1A), large complexes of mRNA and protein that block mRNA degradation and translation (Cassola *et al.*, 2007; Cassola, 2011). In parasites from an early/mid log phase of growth, TcUBP1 is distributed with a speckled pattern throughout the cytoplasm and nucleus (Fig. 1B), as previously shown (Cassola *et al.*, 2007; Cassola and Frasch, 2009). These small speckles are TcUBP1 RNP complexes, which might have different protein composition, and that condense into mRNA granules under nutrient limitation stress (Cassola, 2011). Usually, RBPs are found in the soluble fraction after cell rupture and centrifugation at 10000× *g*, which is typically called S10 fraction, whereas the remaining pellet is called P10 fraction. However, in starved parasites, we found TcUBP1 in both insoluble P10 and soluble S10 fractions, whereas in early/mid log parasites, we found it exclusively in the soluble S10 fraction (Fig. 1C). In the P10 fraction of starved parasites, we could also detect TcPABP1 and TcRBP3, both components of mRNA granules (Cassola *et al.*, 2007), although a reduced presence of both proteins could also be detected in the P10 fraction of unstressed parasites. However, in the P10 fraction of either population, we could not detect the ribosomal protein TcL19 or the nuclear RRM-type RBP TcLA, both absent from mRNA granules (Fig. 1C). These two proteins remained exclusively in the soluble S10 fraction as expected. This suggests that the P10 fraction obtained from both populations contain specific cytoplasmic RBPs, among other cellular compo-

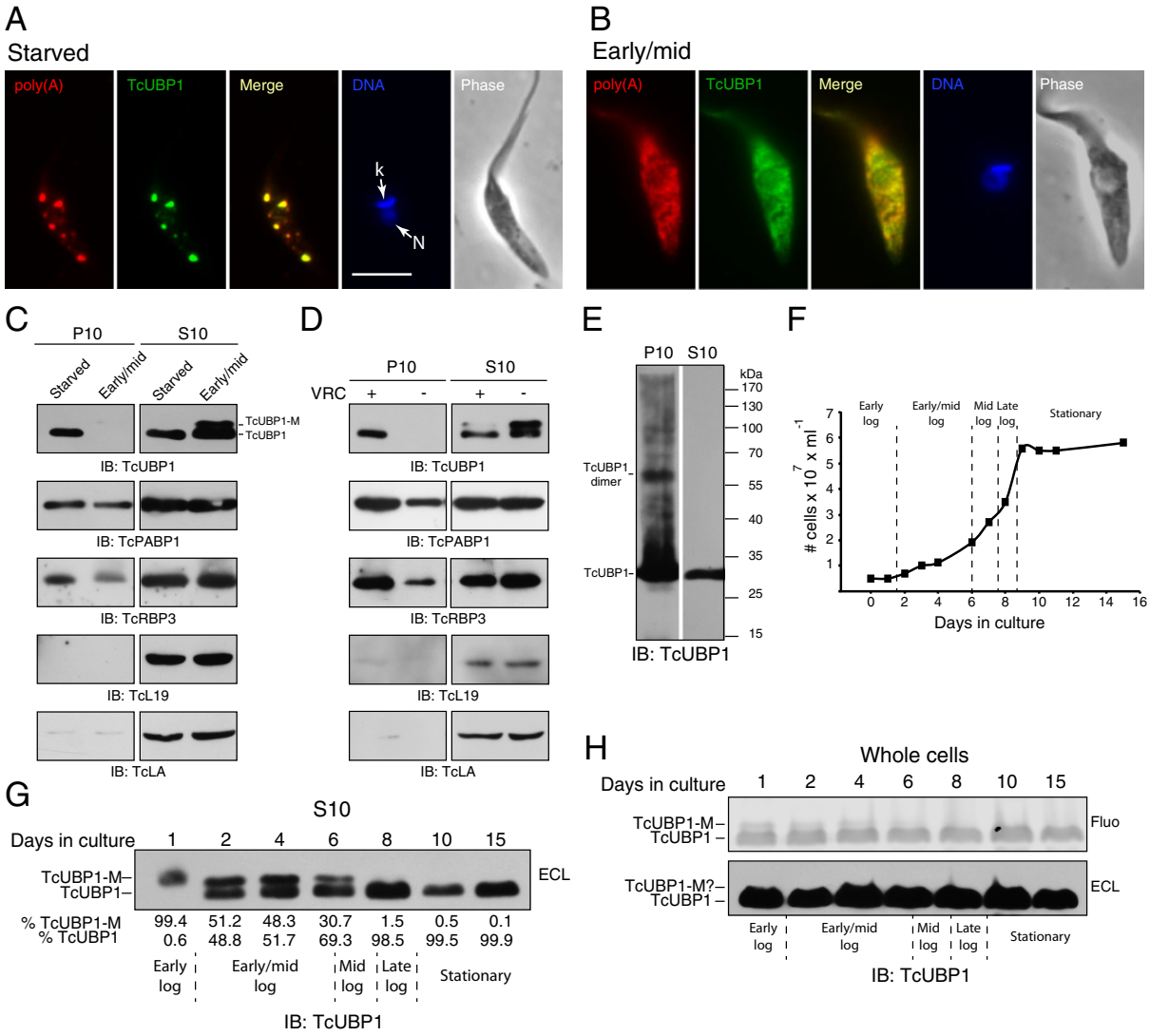

Fig. 1. Condensation of RNP complexes containing TcUBP1 and its posttranslational modification are modulated by growth conditions.
A. Cells under carbon source starvation.
B. Cells in the early/mid log phase were used for localization studies of TcUBP1 together with poly(A) mRNA by FISH. DAPI staining reveals the position of nuclear (*N*) and kinetoplast (*k*) DNA. Scale bar, 5 μm.
C. Parasites under starvation and in the early/mid log phase were used to prepare P10 and S10 samples, and used for Western to detect TcUBP1, TcPABP1, TcRBP3, TcL19 and TcLA in each sample. TcUBP1 corresponds to the faster migrating protein band, whereas TcUBP1-M corresponds to a modified TcUBP1 form with slower motility.
D. Parasites in the early/mid log phase were used to prepare P10 and S10 samples in the presence or absence of VRC and used to detect the same proteins as in C.
E. Western blot of S10 and P10 protein samples obtained from formaldehyde cross-linked epimastigotes.
F. Growth curve of epimastigotes. Day 0 corresponds to 5×10^7 cells ml^{-1}. The defined growth intervals are depicted in the curve.
G. Western blot of S10 samples from the growth curve detected by enhanced chemiluminescent (ECL) detection of HRP-conjugated secondary antibody. Percentages of each TcUBP1 band are shown for each time point.
H. Western blot of whole cell samples obtained from the same growth curve. Whole cells correspond to parasites boiled in 1× SDS-PAGE sample Buffer. The first panel shows the detection by IRDye 680-conjugated secondary antibody exposed near to saturation intensity. Quantitation of each band was impossible due to contamination of the TcUBP1-M area with smears from TcUBP1. The defined growth intervals are depicted in the Western blots. The color of the obtained image was inverted and converted to gray scale. The following panel corresponds to ECL detection of the same blot. The presence of TcUBP1 and TcUBP1-M is indicated in each panel.

nents, but not polysomes or unrelated RNP complexes, as those composed by the nuclear TcLA protein. For TcUBP1, differential growing conditions could be modulating the degree of condensation of RNP complexes, allowing its differential distribution to soluble and insoluble fractions. In order to determine if the differential fractioning of TcUBP1 to P10 and S10 fractions was due to RNP disassembly, we performed the same fractioning in early/mid log phase parasites in the presence and absence of the ribonuclease inhibitor vanadyl ribonucleoside complex (VRC). Under these conditions, we found half of the amount of TcUBP1 in the P10 and the remaining in the S10 (Fig. 1D). Regarding TcPABP1 and TcRBP3, both showed an increase in the P10 fraction in the presence of VRC (Fig. 1D), with a very similar pattern to that of the P10 of starved parasites. Regarding TcL19 and TcLA, both proteins were not precipitated to the P10 in the presence of VRC, showing that the precipitation of cytoplasmic RBPs is specific and does not seem to involve polysomes (Fig. 1D). Overall, these results show that a pool of TcUBP1, TcPABP1 and TcRBP3 are tethered to an insoluble fraction under conditions of mRNA granules formation in starved parasites. TcUBP1 can be differentially precipitated when RNA is protected from degradation by VRC in early/mid log phase parasites, which do not contain mRNA granules. These insoluble fractions are probably specific RNP complexes, which are not contaminated with ribosomes or unrelated RBPs such as the TcLA protein.

Intriguingly, an additional TcUBP1 band with reduced electrophoretic mobility was detected in the S10 fraction from early/mid log parasites and in the absence of VRC (Fig. 1C and D). This form was denominated TcUBP1-M hereafter due to a possible posttranslational modification. We could not detect TcUBP1-M either in the P10 or S10 fractions of starved parasites (Fig. 1C), suggesting this form is only present in parasites growing with abundant nutrients (see next sections).

From these results, we hypothesized that TcUBP1 in the P10 fraction might be associated with RNA in large RNP complexes, either in mRNA granules from starved parasites, or in uncondensed intact RNP complexes in unstressed parasites. The S10 fraction might contain smaller TcUBP1 RNP complexes, or unbound TcUBP1. To test this hypothesis, we analyzed TcUBP1 fractioning in extracts from formaldehyde-fixed mid log parasites, a treatment that facilitates cross-linking of proteins to RNA in living cells (Niranjanakumari *et al*., 2002). In these samples, we found smears only in the P10 fraction and not in the S10 (Fig. 1E), indicative of cross-linked TcUBP1/RNA and TcUBP1/protein complexes. A putative TcUBP1 homodimer was detected in cross-linked samples as a single and abundant band of around 60 kDa (Fig. 1E). We have previously shown this conformation for TcUBP1 (D'Orso and Frasch, 2002). In short, these results show that TcUBP1/RNA complexes from early/mid log phase parasites fractionate to the insoluble P10 fraction even in the absence of large mRNA granules.

Regarding the TcUBP1-M form, its detection in parasites from the dissimilar growth conditions shown in Fig. 1C made us analyze its presence in parasites at different densities of growth, in order to gain insight into its nature. Aliquots from a growth curve (Fig. 1F) were taken at different time points and used to prepare S10 and whole cell samples (obtained after boiling parasites in SDS-PAGE Cracking Buffer), in which we analyzed the presence of TcUBP1 forms after Western blot. In the S10 sample from day one in culture, we found TcUBP1-M exclusively (Fig. 1G). In aliquots from days 2, 4 and 6, corresponding to an early/mid log phase of growth, we found a mixed population of both forms. Instead, in aliquots from days 8, 10 and 15, corresponding to late log and stationary phases of growth, we found TcUBP1 exclusively (Fig. 1G). In whole cell samples from the same aliquots, we detected TcUBP1-M in parasites from the early and early/mid log phase of growth, but not in the mid/late/stationary phases of growth (Fig. 1H). Here, TcUBP1 detection was performed with a fluorescently labeled secondary antibody that gave a high signal-to-noise ratio and wide linear dynamic range (Gingrich *et al*., 2000). Enhanced chemiluminescence (ECL) detection of the same blot gave thick TcUBP1 bands that masked TcUBP1-M due to the high signal of TcUBP1 (Fig. 1H). Testing other parasite treatments like heat shock, oxidative stress, or transcription inhibition did not lead to higher *in vivo* TcUBP1-M levels (not shown). Our results suggest that TcUBP1-M is an endogenous form that is detectable only in parasites growing under high-nutrient and low-density conditions; under these conditions TcUBP1-M can increase its levels after cell rupture, probably as a result of disassembly RNP complexes. Collectively, these results show that nutrient availability modulates the degree of TcUBP1 RNP complexes condensation and precipitation, which correlates with the detection of TcUBP1-M levels.

A screening for modulators of TcUBP1 RNA-binding identifies TcP22

Previously, we have determined that TcUBP1 is associated with mRNA through its RRM both *in vivo* and *in vitro* (D'Orso and Frasch, 2002; Cassola *et al*., 2007). Aiming at the identification of putative TcUBP1 interacting proteins that could modulate its association with RNA, we conducted a biochemical screening for proteins that could associate with TcUBP1 RRM. To accomplish this, we performed an affinity chromatography using immobilized TcUBP1 RRM fused to GST (GST-ΔNΔQG2 construct comprising amino acids 35–126) or unfused GST as a

negative control, followed by mass spectrometry analysis. In this way, we aim to identify only those interactions between the RRM of TcUBP1 and not with other parts of the molecule. We used an RNA-depleted protein extract as a source for protein ligands, which allowed the identification of direct protein–protein interactions and not those mediated by RNA. As a result, we obtained a discrete protein band that was clearly absent in the GST control chromatography and that corresponded to TcP22 protein precursor (TcCLB.509965.290) (Fig. 2A).

TcP22 possesses a characteristic mitochondrial acidic matrix proteins (Mam33) domain comprised between amino acids 104–224 according to Pfam database (http://pfam.xfam.org) (Fig. 2B). Mam33 family proteins have been identified in several organisms, which include *T. brucei* P22 and human P32 (Jiang *et al*., 1999; Hayman *et al*., 2001; Sprehe *et al*., 2010). All these proteins share structural topology and have thus been designated as orthologous proteins (Sprehe *et al*., 2010). Human P32 was identified as a binding partner of the splicing factor SF2/ASF (Krainer *et al*., 1991) and of the globular head complement factor 1q on the cell surface, C1QBP (Ghebrehiwet *et al*., 1994). Sequence identity analysis revealed human P32 also corresponds to Hyaluronan-binding protein 1 (Deb and Datta, 1996), revealing its multifunctional nature. To avoid confusions, hereafter we will refer to the human ortholog as P32. In *T. brucei*, the mature TbP22 amino terminus has been mapped to Val 47 (Fig. 2C) (Hayman *et al*., 2001). In our mass spectrometric identification of TcP22, we could not detect peptides corresponding to the first 62 residues, having covered 42% of the protein by identified peptides (Fig. 2C). This suggests that TcP22 could have a similar cleaved signal peptide as its *T. brucei* ortholog. Consequently, we cloned a mature form of TcP22 starting at Ala 44 just after an initial Met, and expressed TcP22 as a His-tagged recombinant protein (rTcP22). This highly purified recombinant protein, which contained no significant contaminating bacterial proteins (Fig. S1), was used to raise antibodies against TcP22 in order to validate the protein–protein interactions. As expected, TcP22 was only recognized in the GST-ΔNΔQG2 eluate and not in the GST one (Fig. 2D). This antibody recognized a single band in soluble S10 protein extracts, showing high specificity (Fig. 2D). TcP22 is expressed in all developmental stages [epimastogotes, cell-derived trypomastigotes and amastigotes (Fig. 2E)], suggesting a functional role throughout the parasite's life cycle.

To determine TcP22 localization, we performed immunofluorescence analyses using the specific TcP22 antibody together with Mitotracker Red CMRos in early/mid log phase epimastigotes. Microscopic analysis of parasites showed endogenous TcP22 is distributed throughout the cell, with certain areas colocalizing with mitochondrial staining but not confined to that organelle (Fig. 2F). Trypanosomes have a single large and tubular mitochondrion (Schneider *et al*., 2008). The mixed localization of TcP22 is in agreement with reports from human P32, which is present in mitochondria (Muta *et al*., 1997; Dedio *et al*., 1998), but also in the nucleus (Majumdar *et al*., 2002; Heyd *et al*., 2008), cytoplasm (Berro *et al*., 2006; Heyd *et al*., 2008) and outer membrane (Ghebrehiwet *et al*., 2014). Colocalization of endogenous TcP22 and TcUBP1 was observed in some foci (Fig. 2F), opening the possibility of an *in vivo* interaction between both proteins. However, we could not detect colocalization between TcUBP1 and TcP22 in starved parasites (Fig. 2G), suggesting that colocalization of both proteins might also be modulated by growth conditions. To confirm the interaction between both endogenous proteins, we performed immunoprecipitation studies using mid log phase epimastigotes and the TcUBP1 antibody, after which we analyzed the presence of TcP22 in the immunoprecipitate. As expected by the colocalization studies, a small amount of TcP22 was immunoprecipitated together with TcUBP1 but not in the normal rabbit serum control (Fig. 2H). As a control, we detected TcPABP1, which forms a complex with TcUBP1 in the cytoplasm of *T. cruzi* (D'Orso and Frasch, 2002). As a specificity control, we performed the reciprocal immunoprecipitation with the anti-TcP22 serum and found TcUBP1-M in the precipitate (Fig. S2). This would mean that TcP22 could coimmunoprecipitate TcUBP1-M, although this was the only form present in the flow through material (Fig. S2). To sum up, we have identified TcP22 as a binding partner of TcUBP1, both by affinity purification and immunoprecipitation of endogenous proteins.

Overexpression of TcP22 decreases the number of TcUBP1 granules in vivo

To get insight into the possible role of TcP22 regulating TcUBP1 association with RNA granules, we overexpressed full-length and mature TcP22 proteins from the inducible pTcINDEX vector (Taylor and Kelly, 2006), both tagged with a C-terminal flag tag. For full-length TcP22-flag (TcP22FL-flag), we obtained an out of the ordinary localization in tetracycline-induced cells (Fig. S3). These parasites showed big accumulations of the recombinant protein in undetermined compartments of the cell that did not colocalize with TcUBP1. The mature form of TcP22-flag (TcP22M-flag) had a localization pattern that was very similar to the localization of endogenous TcP22 (Fig. 3A), with many foci colocalizing with TcUBP1. The detection of TcP22M-flag by Western blot with anti-flag or anti-TcP22 antibodies showed the correct induction of the recombinant protein expression by tetracycline (Fig. 3B). However, this was the result of few cells expressing high

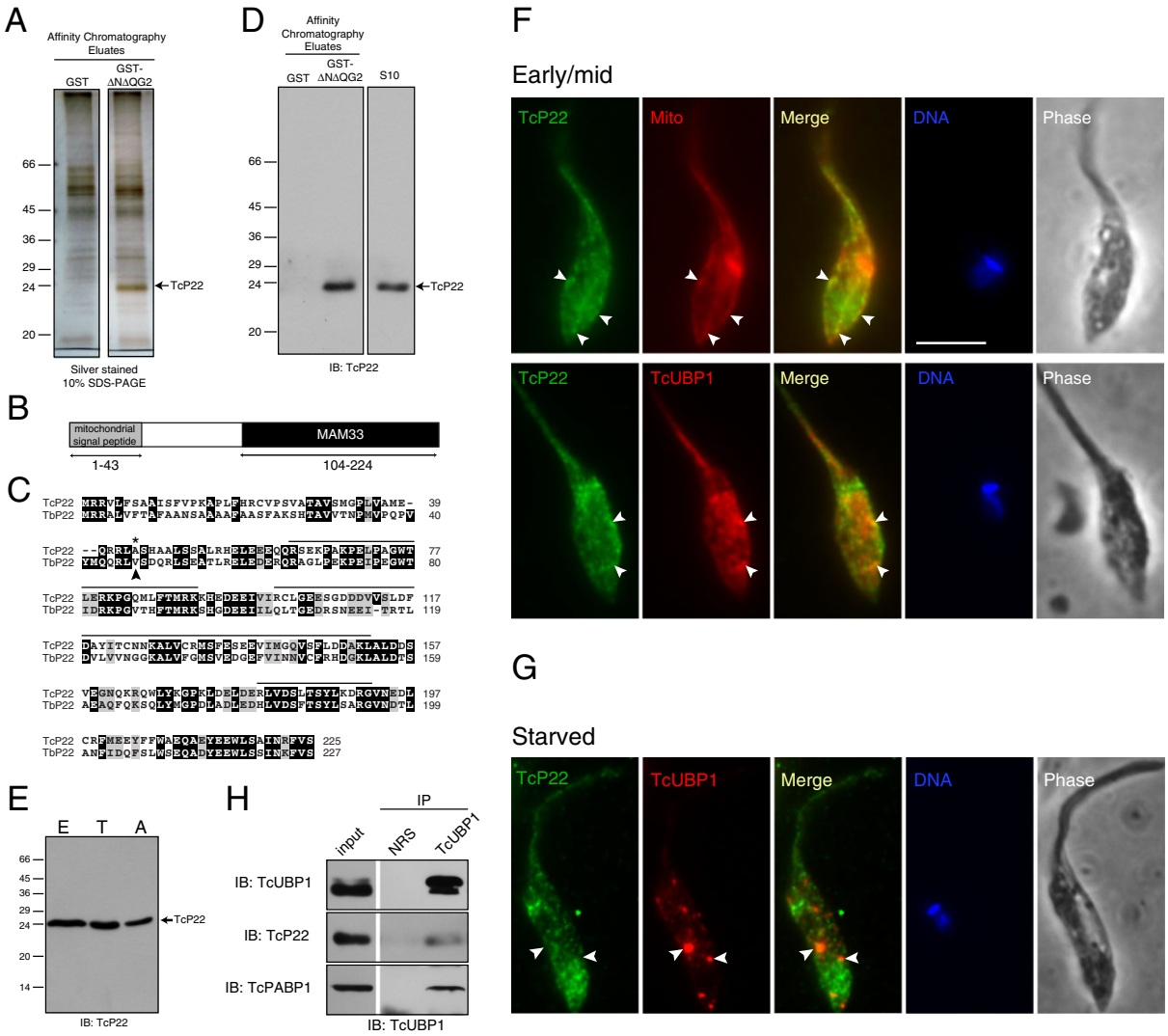

Fig. 2. Identification of TcP22 as an interactor of TcUBP1 RRM.
A. Silver stained SDS-PAGE showing the third eluted fractions from control (GST) and ligand (GST-ΔNΔQG2 construct corresponding to the RRM) from affinity chromatography columns. The position of TcP22 is shown on the gel slice submitted to mass spectrometry.
B. A scheme of TcP22 showing the sequence coverage of the putative amino-terminal mitochondrial signal peptide and the characteristic MAM33 domain as identified by PFAM (http://pfam.xfam.org).
C. Sequence alignment of TcP22 and TbP22 performed by Clustal W algorithm. Identical residues are boxed in black, whereas similar residues are boxed in gray. An arrowhead marks the position of the experimentally determined mature protein in TbP22, whereas an asterisk marks the position of TcP22 predicted mature protein. Black lines mark the coverage of TcP22 identified peptides by mass spectrometry.
D. Western blot to detect TcP22 in the eluted fractions and on a S10 soluble protein extract corresponding to 2×10^7 epimastigotes using specific polyclonal antibodies.
E. Western blot showing the expression of TcP22 on different life forms. E, epimastigote; T, cell-derived trypomastigotes; A, amastigotes. Each lane contains 3, 6 and 3×10^7 cells respectively.
F. Colocalization of TcP22 with the mitochondrion and TcUBP1 in early/mid log phase epimastigotes using specific antibodies and Mitotracker Red CMRos (Mito). Arrowheads mark the position of foci where colocalization of TcP22 with mitochondria or TcUBP1 is evident. DAPI staining reveals the position of nuclear and kinetoplast DNA. Scale bar, 5 μm.
G. Localization of TcP22 and TcUBP1 in starved parasites. Arrowheads mark the position of TcUBP1 RNA granules devoid of TcP22.
H. Western blot using specific antibodies to detect immunoprecipitated TcUBP1 and coimmunoprecipitating proteins. NRS corresponds to normal rabbit serum. We used 1%, 3% and 1% of S10 extracts as material for input samples, and 1/10, 1/3 and 1/5 of immunoprecipitated samples for immunoblots to detect TcUBP1, TcP22 and TcPABP1 respectively. S10 extracts for immunoprecipitation were prepared from mid log phase epimastigotes.

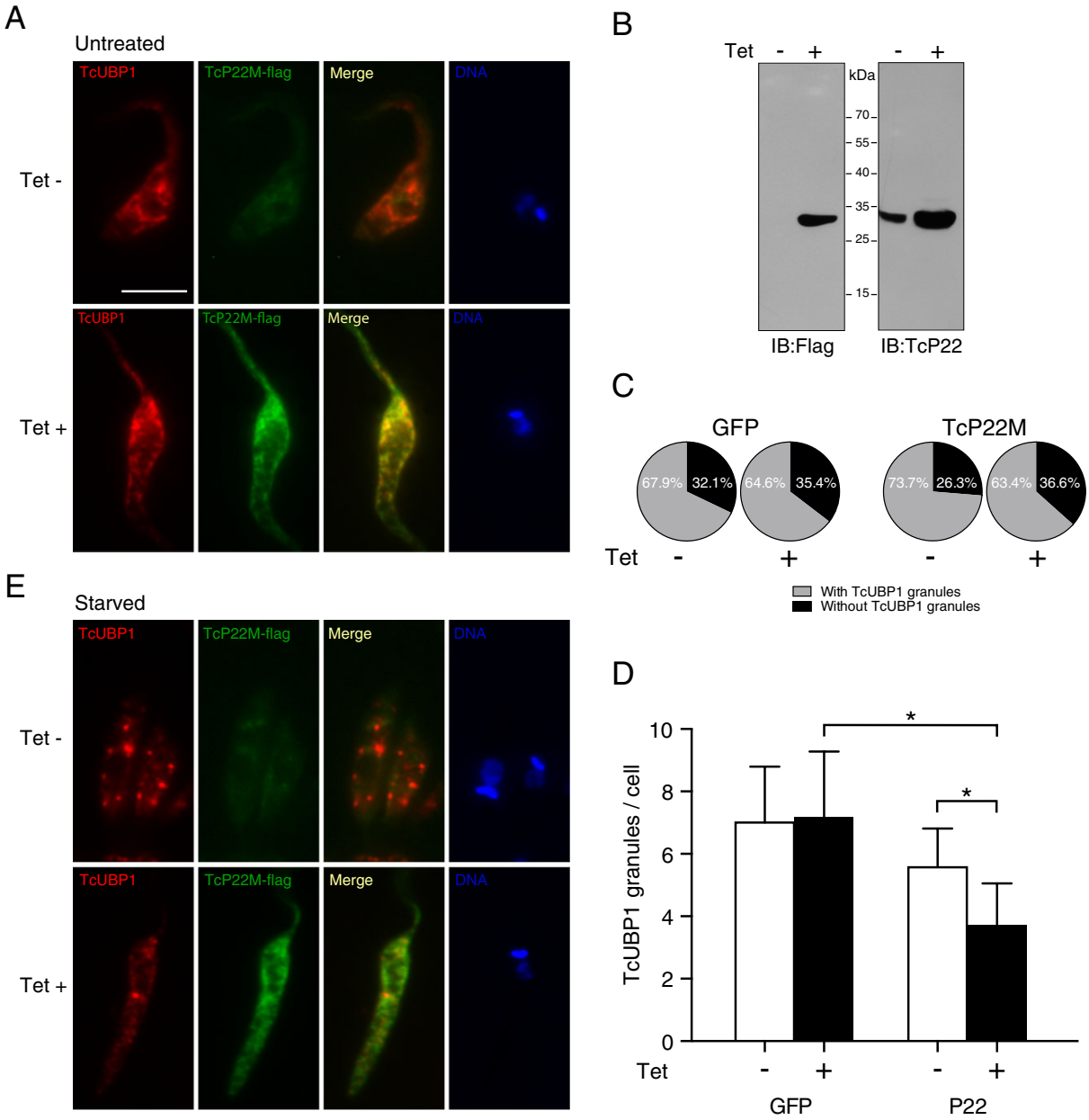

Fig. 3. TcP22M overexpression diminishes the number of TcUBP1 granules under starvation stress.
A. Localization of endogenous TcUBP1 and TcP22M-flag was performed in control uninduced and tetracycline-induced transgenic parasites.
B. Uninduced or tetracycline-induced transgenic parasites transfected with TcP22M-flag from the pTcINDEX vector were processed for Western blot to detect TcP22M-flag with the anti-flag M2 monoclonal antibody. The blot was stripped and used to detect TcP22 with the anti-TcP22 mouse polyclonal antibody.
C. Analysis of the presence or absence of TcUBP1 granules in uninduced or tetracycline-induced parasites transfected with pTcINDEX-GFP or pTcINDEX-TcP22M-flag.
D. Analysis of the amount of TcUBP1 granules per parasite in uninduced or tetracycline-induced pTcINDEX-GFP or pTcINDEX-TcP22M-flag transfected cells.
E. Localization of endogenous TcUBP1 and TcP22M-flag was performed in uninduced and in tetracycline-induced transgenic parasites subjected to starvation stress for 24 h.

amounts of TcP22M-flag (Fig. S4A). This was also the case for GFP (Fig. S4B). This variability has already been described in the original pTcINDEX vector report using clonal populations (Taylor and Kelly, 2006). Parasites transfected with TcP22M-flag and GFP in pTcINDEX were analyzed for the presence and number of TcUBP1 granules before and after induction, under starvation stress. We did not find an important difference between the numbers of parasites with TcUBP1 granules before and after TcP22M-flag overexpression, or when comparing parasites overexpressing TcP22M-flag and GFP (Fig. 3C). However, we did observe a lower number of TcUBP1 granules in parasites overexpressing TcP22M-flag as compared with uninduced parasites or with parasites overexpressing GFP (Fig. 3D and E, Fig. S4C and D). We found no TcP22M-flag in TcUBP1 granules, as already shown in Fig. 2G. This suggests that if TcUBP1 is associated to RNA in granules, it might not be able to interact with TcP22M. Overall, these results suggest that TcP22M might impede the association of TcUBP1 to ribonucleoprotein complexes and granules *in vivo*.

Functional interplay between TcP22 and TcUBP1-RNP complexes

To gain further insight into the possible role of TcP22 as a regulator of TcUBP1 association to RNA granules, we analyzed whether rTcP22 could release TcUBP1 from endogenous RNP complexes using the differential fractioning of TcUBP1. First, we performed the S10/P10 fractioning in the presence of rTcP22, VRC or both in starved parasites. We found that rTcP22 could reduce the amount of TcUBP1 in the P10 fraction in the absence of VRC (Fig. 4A, lane 2), while it could also release a pool of TcUBP1 molecules into the S10 in the presence of VRC (Fig. 4A, lane 4). Second, in early/mid log phase parasites, we observed a marked release of TcUBP1 from the insoluble P10 fraction induced by rTcP22 (Fig. 4A, compare lines 7 and 8), with the concomitant increased detection of TcUBP1-M. In a control experiment, we saw no effect of rTcP22 on the fractioning of TcPABP1 or of the ribosomal protein TcL19 (Fig. S5), suggesting that TcP22 effect is specific for TcUBP1. Furthermore, the addition of GST, as an unrelated recombinant protein control, showed no differences in TcUBP1 fractioning, showing the specificity of this observation (Fig. S5). These experiments show that rTcP22 can promote the solubility of TcUBP1, suggesting TcUBP1 is released from endogenous RNP complexes.

We next tested whether the putative modification on TcUBP1-M promoted by rTcP22 could have an effect on TcUBP1 reassociation to RNA. For this experiment, we used mid log phase epimastigotes in order to obtain both TcUBP1 forms in the S10 after rTcP22 addition, either in the absence or in the presence of VRC. First, we verified that when RNA was protected from degradation by VRC TcUBP1 was found in the P10 fraction as expected, whereas the remaining S10 fraction only contained a small amount of TcUBP1 (Fig. 4B, lane 1). Second, in the absence of VRC TcUBP1 was much more abundant in the S10 as expected, and a minor amount could be detected in the P10 (Fig. 4B, lane 5). Addition of rTcP22 shifted TcUBP1 from the P10 fraction to the S10 fraction in a dose dependent manner (Fig. 4B). This change in TcUBP1 RNP complexes precipitation was evident in all samples, although it was more evident in samples containing VRC. We detected TcUBP1-M exclusively in the soluble S10 fractions and not in the precipitated P10. TcUBP1-M levels increased with the amount of rTcP22 added (Fig. 4B). This was verified in a control experiment where TcUBP1-M levels were dependent on the amount of rTcP22 added (Fig. S6). Third, we used these S10 fractions containing TcUBP1 and TcUBP1-M in binding reactions with homopolymeric RNAs, allowing us to study the effect of this putative modification in *in vitro* RNA-reassociation studies. In this assay, poly(U) RNA in excess is expected to bind endogenous TcUBP1, whereas poly(A) RNA serves as a background control. As shown in Fig. 4C, both TcUBP1 and TcUBP1-M could bind to poly(U) RNA specifically. Here, it should be taken into account that samples from poly(U) eluates that lacked TcUBP1 was due to its sequestering into the corresponding P10 fraction. Regarding TcUBP1-M amounts, these were higher in eluates and flow trough fractions than in the original S10 fraction (Fig. 4C). Interestingly, in eluates from poly(U) RNA-binding assays, we systematically observed a higher level of TcUBP1 compared with TcUBP1-M (Fig. 4C). This difference was not reflected in the corresponding flow through samples (see Fig. 4D for a comparative analysis between eluates and flow through samples). This might imply that TcUBP1 associates more efficiently with poly(U) RNA than TcUBP1-M and that TcUBP1-M has reduced binding capacity. We propose that rTcP22 can promote the dissociation of TcUBP1 from endogenous RNP complexes, thus allowing a putative posttranslational modification that reduces TcUBP1 reassociation with RNA.

We have shown that preserving RNA integrity with VRC prevents TcUBP1-M detection (Figs 1D, 4A and B), suggesting that this posttranslational modification only occurs on unbound TcUBP1. Then, other ways to promote TcUBP1 free state would raise TcUBP1-M levels in cell-free extracts. To gain insight on this question, we prepared S10 extracts with different additives and treatments from early/mid log phase epimastigotes. In S10 samples with no additives, we obtained high TcUBP1-M levels (Fig. 4E, lane 1). As shown before, the levels of TcUBP1-M correlate to the growth phase of the cells (Fig. 1G). When S10

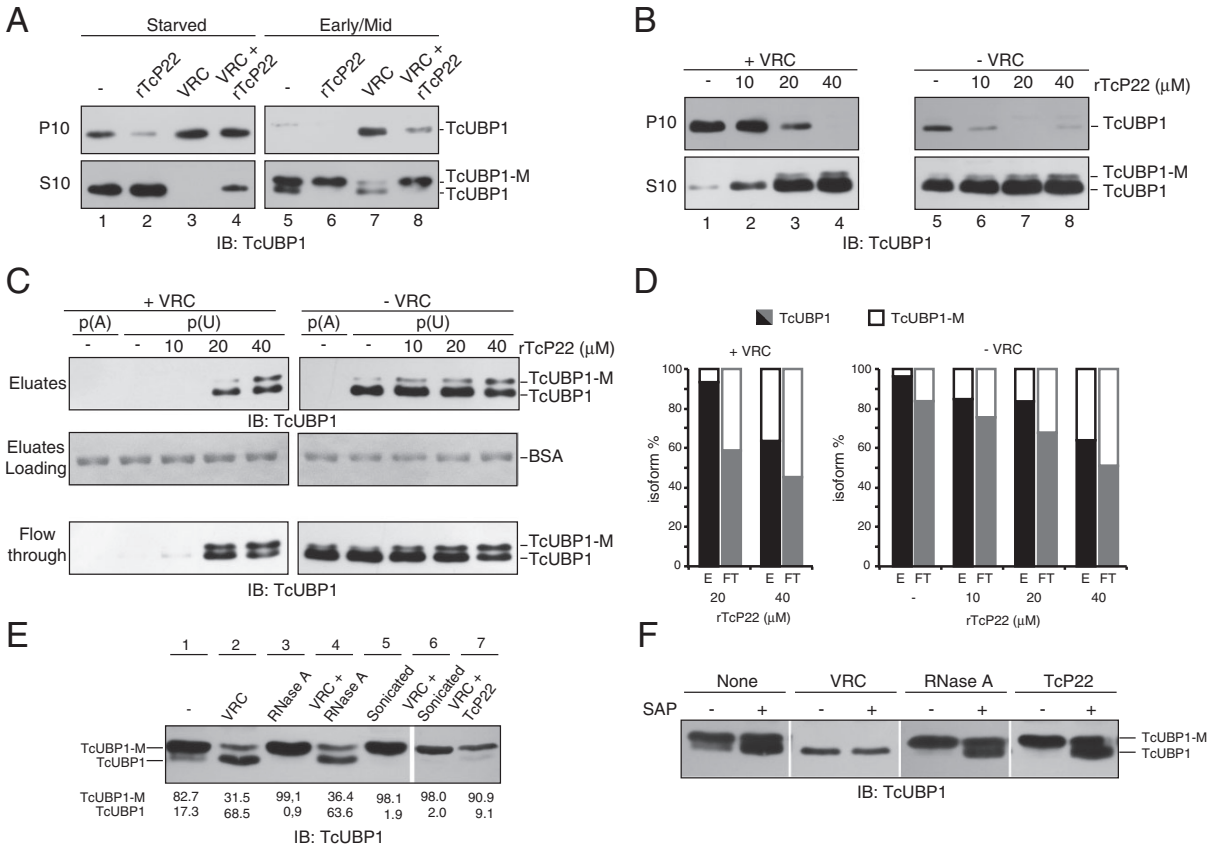

Fig. 4. TcP22 can displace TcUBP1 from endogenous RNP complexes.
A. Western blot of samples from a P10/S10 fractioning from starved or early/mid log phase epimastigotes. Cells were lysed in the presence or absence of rTcP22, VRC or both.
B. Western blot of samples from a P10/S10 fractioning from mid log phase epimastigotes in the presence or absence of VRC and different amounts of rTcP22.
C. Eluates from a protein pull down assay using poly(U), or poly(A) as a control, and the soluble protein extracts (S10) from B. Loading corresponds to the Ponceau staining of BSA from the Binding Buffer present in all eluted samples.
D. Densitometric quantitation of band intensity was performed in the eluates (E) and flow through (FT) fractions from the RNA pull down assay shown in B using ImageStudio Lite software, in order to compare the amount of the different TcUBP1 forms. Only E and FT samples derived from VRC treated extracts with TcP22 at 20 and 40 μM were measured.
E. Western blot of S10 protein extracts prepared in the presence of the mentioned additives or treatments in Lysis Buffer. A dash refers to an extract with no additives. rTcP22 was used at 40 μM. Percentages of the abundance of each TcUBP1 form have been included in the respective lanes.
F. Early/mid log phase epimastigotes were used to prepare S10 extracts in the presence of VRC, RNase A or rTcP22 in SAP reaction Buffer, either in the presence or absence of 2U of SAP.

extracts were prepared in the presence of VRC, we obtained an equally mixed population of TcUBP1 forms (Fig. 4E, lane 2), showing that RNA preservation in the sample prevents TcUBP1 modification. On the contrary, RNase A addition made TcUBP1 form disappear completely (Fig. 4E, lane 3), clearly showing that depleting RNA in the sample leads to complete modification of TcUBP1. As expected, RNase A effect could be prevented by VRC inhibition (Fig. 4E, lane 4), confirming that unbound TcUBP1 suffers this modification. A non-enzymatic way to obtain rupture of RNP complexes is by sonication. This treatment resembled the effect of RNase A but could not be prevented by VRC addition as expected (Fig. 4E, lanes 5 and 6). This shows that the effect of VRC over TcUBP1 modification is specific, as it only blocks RNA degradation but not TcUBP1 modification. As previously shown, rTcP22 promoted the modification of TcUBP1 in the presence of VRC (Fig. 4E, lane 7), suggesting that rTcP22 is not producing RNA degradation *per se*. In a control experiment, RNase A treatment promoted complete TcUBP1 release from the P10 and its modification (Fig. S5, lane 7). However, RNase A treatment had only a small effect over TcPABP1 in the P10 (Fig. S5). On the contrary, we found the ribosomal protein

TcL19 in the precipitated fraction in these samples (Fig. S5, lane 7). The precipitation of TcL19 could be due to ribosomal protein aggregation in the absence of ribosomal RNA (Maximiliano Juri Ayub, personal communication). If this is the case, then rTcP22 is not promoting RNA degradation as there is no precipitated TcL19 when rTcP22 is added (Fig. S5, lane 4). This argues against a possible contamination with ribonucleases of our rTcP22 preparations, which only contained the single protein band of rTcP22 (Fig. S1).

In order to determine if TcUBP1-M corresponds to a phosphorylated form, we first used shrimp alkaline phosphatase (SAP) to treat S10 extracts from early/mid log phase epimastigotes prepared in the presence or absence of VRC, RNase A or rTcP22. This approach would allow the dephosphorylation of a phosphorylated TcUBP1 form, and its detection by Western blot. In this experiment (Fig. 4F), TcUBP1 and TcUBP1-M levels in untreated extracts were similar to those of Fig. 4E. SAP treatment produced an increase in the amount of TcUBP1 form (Fig. 4F). Extracts prepared in the presence of VRC showed a small amount of TcUBP1 in the S10, but there was no effect upon SAP incubation (Fig. 4F). Extracts prepared in the presence of RNase A or rTcP22 showed TcUBP1-M exclusively, whereas SAP treatment increased TcUBP1 levels in both samples. These data argue that TcUBP1-M corresponds to a phosphorylated form. Altogether, these results support a model where rTcP22, or mRNA degradation, can promote the dissociation of TcUBP1 from RNP complexes, thus allowing TcUBP1 phosphorylation exclusively after detaching from mRNA.

TcP22 interacts with a functional TcUBP1 RRM β-sheet

One of the main findings of this work is that rTcP22 can displace TcUBP1 from endogenous RNP complexes. Since TcP22 was identified as a TcUBP1 RRM interacting protein (Fig. 2A), we conducted the biochemical characterization of this interaction in order to understand it mechanistically. All known TcP22 orthologs have shown to display a trimeric conformation (Jiang *et al*., 1999). We analyzed the quaternary structure of rTcP22 by gel filtration chromatography, from which we obtained a single peak with a molecular mass of 87.9 kDa (Fig. S7A), a size compatible with a trimeric conformation. Alternatively, a cross-linking approach using different Glutaraldehyde (GA) concentrations with rTcP22 resulted in the formation of a predominant complex with a molecular mass compatible with a trimeric form (Fig. S7B). We confirmed that trimeric rTcP22 interacts with GST-TcUBP1 and its RRM (GST-ΔNΔQG2) by GST pull-down assays using cross-linked rTcP22 (Fig. 5A). Given the novelty for this kind of RRM/protein association, it prompted us to elucidate the protein determinants in TcUBP1 that are important for this interaction. For this, we used several TcUBP1 deletion and point mutants in *in vitro* interaction assays. Basically, TcUBP1 consists of a central RRM followed by a short Gly-rich region, and accessory amino and carboxy-terminal LC Gln-rich sequences (Fig. 5B). Our results show that rTcP22 could efficiently interact *in vitro* with TcUBP1, ΔNΔQG1 and ΔNΔQG2 protein constructs (Fig. 5C), being the later the minimal sequence corresponding to the RRM that can bind RNA (D'Orso and Frasch, 2002). However, rTcP22 could not interact with mutΔNΔQG2, an RRM mutant that has R84, Y86 and F88 of the RNP1 conserved motif substituted with alanine residues (Fig. 5C). This mutant protein lacks RNA-binding capacity and the typical TcUBP1 localization to RNA granules (Cassola and Frasch, 2009). rTcP22 could not interact either with the ΔNΔQG2β mutant (Fig. 5C), which has an incomplete β-sheet surface lacking the typical β4 strand. The β4 strand in TcUBP1 RRM forms a β-hairpin involved in RNA-binding (Volpon *et al*., 2005). These results show that rTcP22 can only interact with an intact RRM, and that mutating the RRM β-sheet in different locations prevents the interaction with rTcP22, thus suggesting that the RRM β-sheet is involved in this interaction.

To gain graphical comprehension of the interaction between TcUBP1 RRM and TcP22, we performed *in silico* docking simulations. For this we used the NMR-solved structure of TcUBP1 RRM (Volpon *et al*., 2005). The TcP22 monomer was modeled using the solved crystal structure of the *T. brucei* ortholog (3JV1) as a template (Sprehe *et al*., 2010) (Fig. 5D). Although the trimeric structure obtained by Symmdock resembled a volcano (Fig. 5E and F), ClusPro prediction looked more like a doughnut (not shown). The Symmdock prediction was preferred over ClusPro prediction as the Procheck values were less favorable for the latter. We then predicted the binding orientation of TcUBP1 RRM on the TcP22 trimer obtained by Symmdock (Fig. 5G). This can be seen in the detail in Fig. 5H, showing R84, Y86 and F88 of the RRM in direct contact with the TcP22 trimer. For comparison, the surface of the RRM is shown in a modeled protein/RNA complex using HADDOCK (Fig. 5I), as determined by Volpon *et al*. (2005). Here, residues R84, Y86 and F88 are shown to be in close proximity to the RNA. These predictions support our experimental results providing a comprehensive view of the surfaces involved in the non-conventional association between the TcUBP1 RRM and TcP22.

Overall, the results from this work complement our understanding of the yet poorly understood regulation of RBP function in trypanosomes, giving a deeper view on the decondensation of TcUBP1 RNP complexes from a lax layout into mRNA granules to protect mRNA from

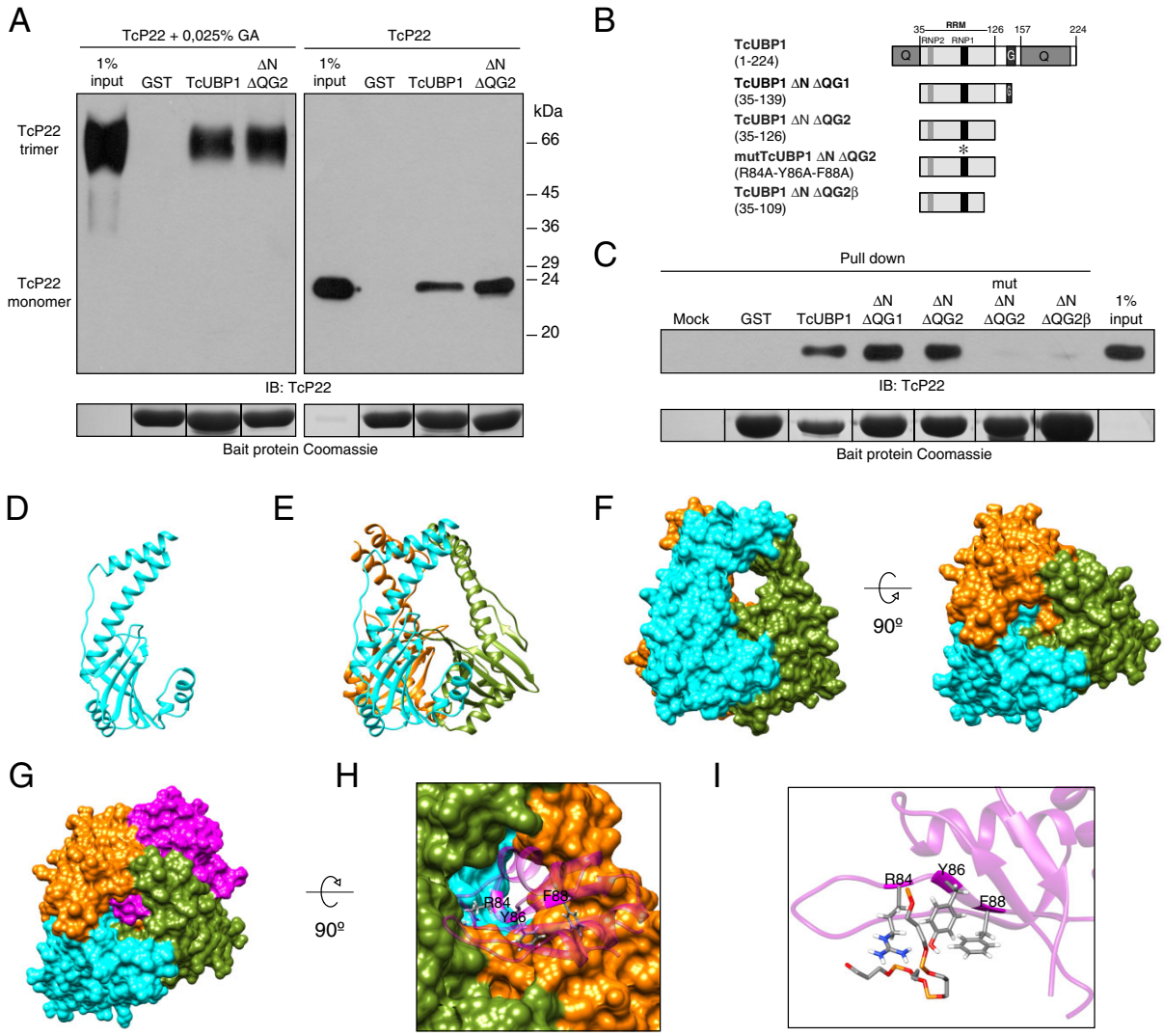

Fig. 5. A functional TcUBP1 RRM β-sheet interacts with a TcP22 trimer.
A. Western blot of GST-pull down eluates using Glutaraldehyde cross-linked or native rTcP22 with GST, GST-TcUBP1 or GST- ΔNΔQG2 (TcUBP1 RRM). Each lane has its own Coomassie blue staining of the GST-fused proteins and rTcP22 input.
B. A domains scheme of the different TcUBP1 protein constructs used in this study.
C. Western blot of GST-pull down eluates using different TcUBP1 mutant proteins. Mock corresponds to a pull down in the absence of GST-fused protein.
D. Modeled tridimensional structure of a TcP22 monomer based on the structure of its *T. brucei* ortholog, TbP22 (PDB 3JV1) using Symmdock.
E and F. Predicted quaternary structure prediction of the TcP22 trimer using Symmdock visualized as ribbons and surface respectively.
G. Docking prediction of TcP22 trimer together with TcUBP1 RRM obtained by using ClusPro.
H. Detailed view of TcUBP1 RRM residues R84, Y86 and F88 in a docking prediction with TcP22 trimer.
I. View of TcUBP1 RRM residues R84, Y86 and F88 during interaction with RNA oligonucleotide 5′-UUUGUUUUUG-3′, obtained by NMR titration (Volpon *et al.*, 2005).

degradation under nutritional stress. Different factors can modulate the reassociation of TcUBP1 to RNP complexes, namely TcP22 and phosphorylation, acting in conjunction in a consecutive manner over TcUBP1 respectively.

Discussion

The central finding derived from this work is that the association of TcUBP1 with RNA can be modulated in *T. cruzi*. The results presented in this work expand our

previous knowledge of RBP dynamics from trypanosomes, parasites of medical importance that mainly rely on the RBP-RNA interplay to modulate gene expression (Fernández-Moya and Estévez, 2010). Previously, we have shown that TcUBP1 can associate with mRNA *in vivo* through the RRM (Cassola *et al*., 2007), thus leaving N- and C-terminal domains available for protein–protein interactions (D'Orso and Frasch, 2002). TcUBP1 C-terminal LC region is divided into Gly and Gln-rich sequences, being the later comprised by 50% glutamines. This disposition resembles aggregation domains containing Gly or polar uncharged amino acids found in other RBPs such as hnRNPA1, TIA-1, TDP-43 and FUS (Ramaswami *et al*., 2013). LC sequences-containing RBPs are often associated with different types of RNA granules implicated in neurodegenerative diseases (Li *et al*., 2013). In fact, reversible precipitation of mRNAs and RNA granule-associated RBPs containing LC sequences could be achieved in a cell-free precipitation assay using a biotinilated isoxazole (Han *et al*., 2012; Kato *et al*., 2012). The precipitation of LC sequences-containing proteins in these samples seemed to be independent on the presence of RNA (Han *et al*., 2012), suggesting that the LC sequences in these proteins were determinant for RNA granule-like formation and precipitation *in vitro*. TcUBP1 granules from parasites under nutrient limitation stress are insoluble in cell-free extracts (Fig. 1C). Under normal conditions mRNA granules are not present in the cell, but TcUBP1 can also be found in the insoluble P10 fraction when mRNA is protected from degradation (Fig. 1D). Different evidences suggest TcUBP1 fractioning to P10 fractions relies on RNA: RNA degradation by RNase prevents TcUBP1 precipitation; and cross-linked TcUBP1/RNA complexes are only detected in the P10, not in the soluble S10 fraction. *In vivo* condensation of TcUBP1 RNP complexes in *T. cruzi* is also modulated by growing conditions (Fig. 1). It seems that the condensation state of RNP complexes containing TcUBP1 also dictate its availability as a phosphorylatable substrate. Although TcUBP1-M *in vivo* levels are significantly reduced when compared with TcUBP1, this modified form could be relevant as a transition state between RNA dissociation and reassociation events. In *T. brucei*, ZC3H11 (Droll *et al*., 2013), ZC3H12 and ZC3H13 (Ouna *et al*., 2012) were reported to be phosphorylated among others (Nett *et al*., 2009; Urbaniak *et al*., 2013), opening new avenues for post-translational modification of RBPs as regulatory mechanisms in trypanosomes. Under high density growing conditions, or starvation, TcUBP1 might not be available for phosphorylation due to recruitment to mRNA granules, or due to ATP shortage. Hence, dephosphorylated TcUBP1 is supposed to stay bound to its target mRNAs until disassembly of mRNA granules or RNP complexes. Under low density growing conditions, with wide availability of nutrients, TcUBP1 RNP complexes are not prone to condensation *in vivo*. Thus, laxer TcUBP1 RNP complexes would make them more permeable to disassembly or degradation, allowing TcUBP1 phosphorylation. This would suggest that dissociation of TcUBP1 from mRNA targets is faster in parasites from the early/mid log phase of growth than in stationary phase parasites. This conclusion is indeed supported by an increased mRNA half-life in stationary phase versus early log phase *T. cruzi* parasites (Cevallos *et al*., 2005). Also, a recent comparative analysis between early and log phase *T. brucei* procyclic cells revealed differential mRNA half-lives between the two conditions (Fernandez-Moya *et al*., 2014), supporting a differential role of RBPs in the posttranscriptional regulation of their transcripts.

A potential way to regulate TcUBP1 association with RNA is through interaction with its RRM. In our RRM interaction screening, we found TcP22, the *T. cruzi* ortholog of human P32. The TcUBP1-TcP22 interaction seems to take place with a subset of molecules in defined foci (Fig. 2F), reflecting why only a limited amount of protein can be immunoprecipitated *in vivo* (Fig. 2H). This makes sense for a protein like TcUBP1, which is supposed to be attached to mRNA molecules most of the time. However, this interaction does not seem to take place in starved parasites, as TcP22 does not localize to TcUBP1-containing mRNA granules. *In vivo* overexpression of TcP22M-flag did not show a notorious change in the number of parasites with TcUBP1 granules but rather we found differences in the number of granules per cell. This could be suggesting that TcUBP1 cannot be recruited efficiently to mRNA granules in these cells. However, it remains to be determined if mRNA granules devoid of TcUBP1 are indeed formed in these cells. In mammalian cells, besides from viral proteins, overexpressed proteins under study usually induce the formation of stress granules. One of the exceptions is isoform 2 of Dishevelled (Dvl2), which has been shown to interact with G3BP while negatively affecting its SG-nucleating activity (Sahoo *et al*., 2012). In our model, it is yet uncertain if TcUBP1 *per se* has mRNA granule nucleating activity.

Remarkably, rTcP22 could prevent TcUBP1 precipitation from endogenous mRNA granules and RNP complexes (Fig. 4), but independently of RNA degradation (Fig. S5). This would suggest that it can interact with TcUBP1 in a fashion that affects its binding to RNA, thus releasing it from the RNP. Murine P32 was reported to bind RNA *in vitro* (Yagi *et al*., 2012), which could explain TcP22 competition for the RNA itself and not for the RRM of TcUBP1. However, we have not been able to detect direct rTcP22 binding to RNA *in vitro* (data not shown), similarly to what has been reported for *T. brucei* P22 (Hayman *et al*., 2001).

The release of TcUBP1 from endogenous RNP complexes results in its phosphorylation (Fig. 4F). From our results, we propose that this modification might have a direct negative impact on the association of TcUBP1 with its target RNAs. Recently, Singh *et al*. used yeast two-hybrid and TAP-tag affinity chromatography approaches to identify a protein kinase that interacts with MKT1, an mRNA metabolism-related protein in *T. brucei* (Singh *et al*., 2014). In another report from *T. brucei*, Cristodero *et al*. found an Arginine N-methyltransferase associated to SCD6, a P-body and mRNA granules component (Cristodero *et al*., 2014). Thus, protein kinases and other protein-modifying enzymes are probably also components of RNP complexes in trypanosomes and might have a role in RNP remodeling as in mammalian cells (Lee and Lykke-Andersen, 2013). Han *et al*. demonstrated that phosphorylation of FUS LC sequence inhibits its association with homotypic hydrogel droplets (Han *et al*., 2012). An alternative explanation for the lack of TcUBP1 phosphorylation in starved parasites could be that growth conditions also modulate kinase activity in *T. cruzi*. Recently, Chung *et al*. showed in *T. cruzi* cells that eIF5A is phosphorylated in Ser and Tyr residues in exponentially growing cells, whereas extensive dephosphorylation occurs in cells from stationary phase (Chung *et al*., 2013). In *Leishmania* and *T. brucei*, components of the eIF4F complex are also differentially phosphorylated during growth phase in culture (Pereira *et al*., 2013).

The characterization of this RRM–protein interaction revealed TcP22 could interact with TcUBP1 RRM β-sheet surface (Fig. 5). Biochemical and *in silico* modeling of the complex provided insight on how a TcP22 trimer could influence TcUBP1 dissociation from endogenous RNP complexes and leading to an RNA-unbound state. Although this interaction seems unconventional, there is growing evidence supporting the involvement of RRMs in protein–protein interactions (Cléry and Allain, 2012). Mammalian PABPC1 RRM1+RRM2 or RRM3+RRM4 interact with importin alpha while free of RNA (Kumar *et al*., 2011). One of the earliest suggestions of RRM–protein interactions was that of SF2/ASF with P32. In this report, P32 could prevent binding to RNA of SF2/ASF and of a ΔRS mutant composed exclusively by RRM1+2 (Petersen-Mahrt *et al*., 1999). This would suggest that P32 interacts with one or both RRMs and not with the RS domain, but the precise protein moieties and amino acids involved in this interaction have not been characterized (Petersen-Mahrt *et al*., 1999). In the case of TcUBP1 and TcP22, we show that the interaction is dependent on the same surface and residues used for RNA binding. This would suggest that P32 itself and its orthologs are potential RRM-binding proteins. In fact, proteomic analysis of the human P32 interactome revealed the presence of twelve RRM-containing proteins, which are mainly involved in nuclear RNA splicing (Zhang *et al*., 2013). However, P32 and its orthologs not only interact with RRM-containing proteins, but also with other kinds of RBPs and many different proteins (Zhang *et al*., 2013). It could be hypothesized that P32–protein interactions might provide momentary associations to redirect interactions in a time and space specific manner. Alternatively, these associations might provide additional support for other interactions to take place, or to enhance them. This is the case of P22 with RBP16 in *T. brucei*, where the binding of P22 to a Cold Shock Domain in RBP16 enhances this RBP association to gRNA in the mitochondrion (Hayman *et al*., 2001; Miller and Read, 2003). The P22–RBP16 interaction seems to be unstable or occurring with only a limited amount of P22 molecules, as it cannot be obtained by *in vivo* immunoprecipitation (Sprehe *et al*., 2010). However, TbRGG2, an RNA-editing factor from *T. brucei*, can be indeed immunoprecipitated (Sprehe *et al*., 2010), suggesting P22 interacts with many different factors *in vivo*. In *T. brucei*, these interactions seem to be important for k-RNA editing, primarily as a COII-specific editing factor (Sprehe *et al*., 2010).

Numerous reports have detected human P32 in the mitochondria (Muta *et al*., 1997; Dedio *et al*., 1998; Yagi *et al*., 2012), whereas others have detected it in numerous other locations (Majumdar *et al*., 2002; Berro *et al*., 2006; Heyd *et al*., 2008; Ghebrehiwet *et al*., 2014). Here, we have used specific antibodies to detect endogenous TcP22 in *T. cruzi*, showing it is distributed throughout the cell including mitochondria (Fig. 2F). It seems likely that P32 and its orthologs can adopt different cellular locations depending on the cell type and external stimuli. Murine P32 was shown to accumulate in the nucleus of a monocyte/macrophage cell line upon stimulation with a mitogen (Majumdar *et al*., 2002), whereas adenovirus infection of human cell lines also promotes the translocation of P32 from the mitochondria to the nucleus (Matthews and Russell, 1998). P32 has been found to be necessary for nuclear translocation of U2AF26 splicing factor through the interaction with a novel nuclear localization sequence (Heyd *et al*., 2008). Moreover, the human P32 interactome analysis revealed the association to many cytoplasmic and nuclear cellular components (Zhang *et al*., 2013). These evidences argue in favor for extra-mitochondrial localizations and functions for P32 and its orthologs. In trypanosomes, TcP22 is not the first case with a dual localization, as the Cysteine Desulfurase Nfs and the Scaffold Protein Isu have also been detected in the mitochondrion and nucleolus in *T. brucei* (Kovarova *et al*., 2014).

In summary, the results presented here provide insight into the growth phase-regulated modulation of TcUBP1 association with RNA by TcP22, arguing for the comple-

mentary role of a regulatory phosphorylation in the dynamic association of RNP complexes in trypanosomatid parasites.

Experimental procedures

Parasite cultures

Trypanosoma cruzi epimastigotes, strain CL Brener, were cultured in BHT medium containing brain heart infusion, 0.3% tryptose, 0.002% bovine hemin and 10% heat-inactivated fetal calf serum (BHT 10%) at 28°C. All parasite cultures were performed in plastic flasks without shaking, unless otherwise stated. Early logarithmic (log) grown parasites were defined as 5 to 7 $\times$ 10^6 cells ml^{-1}, early/mid log grown parasites between 8 and 20 $\times$ 10^6 cells ml^{-1}, mid log grown parasites between 2 and 3 $\times$ 10^7 cells ml^{-1}, late log grown parasites between 3 and 5.5 $\times$ 10^7 parasites ml^{-1}, and stationary phase parasites from 5.5 $\times$ 10^7 parasites ml^{-1}. For time course growing curves, a culture with 1.5 $\times$ 10^7 ml^{-1} was used as a starter inoculum for the initial culture starting at 5 $\times$ 10^6 parasites ml^{-1}. Cultures were hand shaken once every 24 h. For nutritional studies, late log parasites were washed in 137 mM NaCl, 4 mM Na2HPO4, 1.7 mM KH2PO4 and 2.7 mM KCl (PBS) and were incubated for 24 h in PBS. For induction of recombinant proteins from the pTcINDEX vector, we incubated the parasites for 48 h in the presence of 0.5 μg ml^{-1} tetracycline. For starvation studies with these parasites, these were washed with PBS and incubated in PBS plus 0.5 μg ml^{-1} tetracycline for 24 h. The analysis of the presence and number of TcUBP1 granules in uninduced cultures was performed randomly in any parasite of the respective population. For tetracycline-induced cultures, only parasites expressing high levels of TcP22M-flag or GFP were used for the analysis. The raw data for the analysis of this experiment is presented in Supplemental Tables II and III.

Protein extracts and Western blot

For all protein extracts, parasites were first washed once with PBS. For Western blot, parasites were lysed for 15 min at 1 $\times$ 10^6 parasites ml^{-1} in TBS plus 0.5% NP-40, with the addition of 100 μM trans-Epoxysuccinyl-L-leucylamido(4-guanidino)butane (E64) and 1 mM Phenylmethylsulfonyl Fluoride (PMSF) (Lysis Buffer). RNase A (Sigma) was added at 1 μg μl^{-1}, Vanadyl Ribonucleoside Complex (VRC) (Sigma) was used at 20 mM. After lysis, samples were centrifuged at 10 000$\times$ g for 10 min at 4°C. The supernatant was designated S10, whereas the pellet fraction was designated P10. P10 fractions were resuspended in 1$\times$ Cracking Buffer (50 mM Tris-HCl pH 6.8; 2% Sodium Dodecyl Sulfate, SDS; 10% Glycerol; 0.1% Bromophenol Blue; 100 mM Dithiothreitol, DTT), immediately boiled for 3 min and afterward treated with DNase I (Sigma) for 15 min at room temperature to reduce DNA viscosity. Whole cell samples were prepared by incubating washed parasites in 1$\times$ Cracking Buffer, immediately boiled for 3 min and treated with DNase I (Sigma) for 15 at room temperature to reduce viscosity. DNase I untreated samples showed the same TcUBP1 pattern of bands as treated samples. For Shrimp Alkalyne Phosphatase (SAP) (Fermentas) treatment, parasites were lysed in Lysis Buffer supplemented with 1 mM DTT, 5 mM $MgCl_2$, and incubated for 30 min on ice with 2U of SAP in a total volume of 50 μl. After the incubation period, the extract was centrifuged and used as mentioned earlier. Parasite cross-linking with formaldehyde was performed essentially as previously reported (Noe *et al*., 2008), using microscopical inspection of the parasites to confirm complete cell disruption. For Western blot, samples were loaded onto 10% SDS-polyacrylamide gels. Gels were transferred to Immobilon-NC transfer membranes (Millipore), probed with rabbit anti-TcUBP1 (1:2000) (Noe *et al*., 2008), mouse anti-TcUBP1 (1:750), rabbit anti-TcPABP1 (1:2000) (D'Orso and Frasch, 2002), rabbit anti-TcRBP3 (De Gaudenzi *et al*., 2003), mouse anti-TcP22 (1:500), rabbit anti-TcL19 (1:2000) (a kind gift from Maximiliano Jury-Ayub), mouse anti-TcLA (1:1000) (Cassola and Frasch, 2009) and anti-flag M2 mouse monoclonal (1:1000) (Sigma) and developed using horseradish peroxidase-conjugated anti-rabbit or anti-mouse (1:8000) antibodies and the Supersignal West Pico Chemiluminescent Substrate (Pierce) according to the manufacturer's instructions. For fluorescent Western blot, we used IRDye secondary anti-rabbit antibody (LI-COR) diluted 1:20 000. Detection was performed using the Odyssey Imaging System (LI-COR). Quantitation of protein bands was performed using Image Studio Lite software (LI-COR).

Affinity chromatography purification

HiTrap N-hydroxysuccinimide (NHS)-activated Chromatography columns (GE Healthcare) were used according to manufacturer's instructions. All the procedure was performed in a cold chamber at 4°C using ice-cold Buffers and solutions, unless otherwise stated. Briefly, solutions containing the purified ligand Glutathione S-transferase (GST)-TcUBP1 RRM domain at 6 mg ml^{-1}, or unfused GST at 9 mg ml^{-1}, were dialyzed ON at 4° C in 0.2 M $NaHCO_3$ pH 8.3, 0.5 M NaCl (Coupling Buffer). For each column, 1 ml of ligand protein was injected very slowly into the column and left at room temperature for 30 min to allow covalent binding. The columns were inactivated with Buffer A (0.5 M ethanolamine, 0.5 M NaCl, pH 8.3) and washed with Buffer B (0.1 M sodium acetate, 0.5 M NaCl, pH 4) in three rounds. Finally, the pH was adjusted by injecting 2 ml of Tris buffered saline (TBS, 50 mM Tris-HCl pH 7.6; 150 mM NaCl). Prior to the affinity chromatography, a mock run was performed in order to wash any remaining GST fusion protein. The columns were equilibrated in TBS. A single S10 protein extract prepared from 3.5 $\times$ 10^9 mid log phase epimastigotes in Lysis Buffer was used. This soluble protein extract was treated with RNase A at 1 μg μl^{-1} for 30 min, diluted to 35 ml in Lysis Buffer and filtered through 0.45 μ filter. The protein extract was used as the input for the GST column, and the flow through was used as the input of the GST-TcUBP1 RRM column, with a flow of 300 μl min^{-1} using a P1 Pump (GE Healthcare). Both columns were washed extensively with TBS (10 ml) until no more protein was detected in the washes as determined by Bradford assay. Finally, elution of bound proteins was achieved with Elution Buffer (0.5 M NaCl, Tris-HCl 50 mM pH 7.6) into four fractions of 1 ml each. For SDS-PAGE, 100 μl of each fraction was precipitated with chloroform and methanol,

and resuspended in 1× Cracking Buffer. After SDS-PAGE, proteins were detected by silver staining, and the band corresponding to TcP22 was subjected to peptide mass fingerprinting by the Mass Spectrometry Service of Institute Pasteur of Montevideo, Montevideo, Uruguay.

Recombinant protein expression, cross-linking, gel filtration and antibody production

Recombinant TcUBP1 and its deletion and mutant versions were obtained as GST fusions in pGEX-2T by polymerase chain reaction (PCR). TcP22 open reading frame was amplified by PCR and cloned into the NdeI and BamHI sites of pET-22b vector, generating a His-tagged fusion. TcP22FL-flag and TcP22M-flag were amplified by PCR using a reverse oligonucleotide where the flag tag coding sequence was added and cloned into the Not I and Cla I sites of pTcINDEX vector (Taylor and Kelly, 2006). GFP was amplified by PCR leaving 5′ Bam HI and 3′ Bgl II sites and cloned into the BamHI site of pTcINDEX. All oligonucleotides sequences are listed in Supplemental Table I. Constructs for recombinant protein expression and purification were transformed in *Escherichia coli* strain BL21. Cultures transformed with pET22b-TcP22 were induced with 0.2 mM isopropyl b-D-thiogalactopyranoside (IPTG) for 3 h at 37° C, whereas TcUBP1 constructs were induced with 0.5 mM IPTG at 18°C O.N. Bacterial cell pellets containing TcUBP1 recombinant proteins were resuspended in TBS supplemented with 0.5% Triton X-100, 1 mM PMSF, 100 μg ml^{-1} DNase I (Sigma) and 100 μg ml^{-1} RNase A (Sigma). For GST, RNase A was omitted from the lysis buffer. After sonication, centrifugation and filtration through 0.45 μM filter, soluble proteins from the supernatant were purified using GST-agarose resin (Sigma). TcP22-His was purified by immobilized-metal affinity chromatography (IMAC) using IMAC buffer (20 mM Tris-HCl pH 8.8, 500 mM NaCl, 30 mM Imidazole, 100 μg ml^{-1} DNase I, 1 mM PMSF). After elution with 15 mM reduced glutathione or 200 mM Imidazole, respectively, the most concentrated fractions of recombinant proteins were pooled and dialyzed against PBS O.N. prior to any usage. The RNA content of all recombinant protein preparations was under the detection limit of 20 ng ml^{-1} as judged by Qubit RNA BR Assay Kit (Life Technologies). For gel filtration analysis, TcP22 was desalted in 50 mM in Sodium Phosphate Buffer pH 5.8 plus 150 mM NaCl and used as input for a Superose 12 column (GE Healthcare), using the same Buffer. Markers used for molecular weight determination were Alcohol Dehydrogenase (150 kDa), Bovine Serum Albumin (BSA) (66 kDa) and Carbonic anhydrase (29 kDa), all from Sigma. For TcP22 cross-linking, dialyzed TcP22 (20 μg) was incubated with different amounts of Glutaraldehyde (GA) at 37°C for 15 min, stopping the reaction with 200 mM lysine for 30 min. For antibody production, TcP22 was injected into mice with Freund's adjuvant three times at 2 week intervals.

Immunoprecipitation

For each immunoprecipitation reaction, 50 μl of protein A-agarose resin was used. The resin was washed and equilibrated in TBS, followed by incubating for 2 h at 4°C with 100 μl of anti-TcUBP1 rabbit serum or anti-TcP22 mouse serum, or normal rabbit or mouse serum in 400 μl of TBS. After extensive washing with TBS, the resin was equilibrated in Binding Buffer (20 mM Tris-HCl pH 7.6, 50 mM KCl, 5 mM $MgCl_2$, 1 mM DTT, 10% glycerol, 0.5 mg ml^{-1} BSA). Parasite S10 protein extracts from 5×10^8 cells were obtained after lysis in Binding Buffer plus 0.5% NP-40, 100 μM E64 and 1 mM PMSF. S10 extracts were incubated for 2 h with the resin at 4°C, washed four times with ice cold Binding Buffer and eluted by boiling in 100 μl of 2× Cracking Buffer.

Immunofluorescence staining, mitotracker staining, poly(A) mRNA FISH and microscopy

For immunofluorescence studies, fixed parasites were permeabilized and blocked for 1 h in Blocking Buffer (0.5% saponin, 2% BSA) supplemented with 2% normal goat serum, followed by a 2 h incubation with rabbit anti-TcUBP1 diluted 1:500, mouse anti-TcP22 diluted 1:250 and anti-flag M2 monoclonal 1:500 primary antibodies in Blocking Buffer. Alexa-488 or Alexa-546 were used as conjugated secondary antibodies at 1:1000 (Molecular Probes). After extensive washing, parasites were stained with 1 mg ml^{-1} 4,6-diamidino- 2-phenylindole (DAPI) and mounted with 3 μl of Fluor Save reagent. For immunofluorescence coupled to FISH, parasites were post-fixed with 4% paraformaldehyde after immunofluorescence and treated as for poly(A) + mRNA FISH as described (Cassola *et al.*, 2007). The mitochondrion was labeled with Mitotracker™ Red CMXRos (Molecular Probes) following the procedure reported by Vassella *et al.* (Vassella *et al.*, 1997). Analysis of subcellular localization was performed in a Eclipse E600 Microscope (Nikon, Tokyo, Japan) coupled to a SPOT RT color camera (Diagnostic Instruments). Merged images were obtained by superimposing the indicated images files in SPOT Software 4.0.9 (Diagnostic Instruments).

Homoribopolymer binding assay

Dihydrazide-agarose RNA cross-linking was performed as described (De Gaudenzi *et al.*, 2003). Beads (50 μl) were equilibrated in 500 μl of Binding Buffer. S10 extracts from 4.5×10^8 mid log phase epimastigotes were used for each binding assay. These parasites were lysed in Binding Buffer with the addition of 0.5% NP-40, 100 μM E64 and 1 mM PMSF, and VRC when stated. Beads were washed four times with 1 ml of Binding Buffer. Elution was done with 2× Cracking Buffer. Samples were resolved by SDS-PAGE followed by Western blot.

GST pull down assay

For each GST pull down assay, we used 30 μl of Glutathione Agarose resin (Sigma) to which 170 μg of dialyzed GST-tagged recombinant proteins was added. After 1 h of incubation at 4°C, the excess of recombinant protein was extensively washed with TBS, and the resin was blocked with GST Pull Down Blocking Buffer (1% BSA in TBS) for 1 h. Without removing GST Pull Down Blocking Buffer, 100 μg of

rTcP22 was added and further incubated for 1 h, followed by five washes with 1 ml of GST Pull Down Wash Buffer (50 mM Tris-HCl pH 7.6, 150 mM NaCl, 10% glycerol, 0.1% Triton X-100). Finally, bound proteins were eluted by incubating with 30 µl of 15 mM reduced Glutathione in GST Pull Down Wash Buffer and processed for Western blot.

TcP22 structure modeling and docking with TcUBP1 RRM

TcP22 model was obtained using CPHmodel 3.2 server (http://www.cbs.dtu.dk), which used TbP22 monomer structure (3JV1) to model the TcP22 monomer (Fig. 5C). The 3D structure of TcP22 was predicted using Symmdock software (Fig. 5C–E), which determines the structure by symmetry (http://bioinfo3d.cs.tau.ac.il). This program uses an algorithm based on geometry, using the asymmetric monomeric unit to assemble it into a cyclically symmetric complex, in this case a trimer. The model was tested using Prockeck in PDBsum (http://www.ebi.ac.uk). A model obtained using ClusPro (http://cluspro.bu.edu) was also analyzed as it gave a similar structure to the *T. brucei* protein. The Symmdock prediction was preferred to ClusPro prediction as the Procheck values were less favorable for the latter (http://www.ebi.ac.uk). We then used the PatchDock server23 (http://bioinfo3d.cs.tau.ac.il/PatchDock) docking server to predict the binding orientation of TcUBP1 RRM on the TcP22 trimer obtained by Symmdock (Fig. 5F and G).

Acknowledgements

We are indebted to Agustina Chidichimo, Liliana Sferco and Berta Franke de Cazzulo for parasite cultures, Maximiliano Jury-Ayub for the anti-TcL19 antibody, Laurie K. Read for invaluable advice on TbP22 biochemistry, and Morten Nielsen for advice on protein modeling and docking. The work described in this article was performed with financial support from the Agencia Nacional de Promoción Científica y Tecnológica (ANPCyT) to AC and ACF. AC and ACF are members of the Research Career of CONICET, and MAR and GC are CONICET Research Fellows. The funders had no role in study design, data collection and analysis, decision to publish or preparation of the manuscript. The authors have no conflict of interest to declare.

References

Berro, R., Kehn, K., de la Fuente, C., Pumfery, A., Adair, R., Wade, J., *et al.* (2006) Acetylated Tat regulates human immunodeficiency virus type 1 splicing through its interaction with the splicing regulator p32. *J Virol* **80:** 3189–3204.

Cassola, A. (2011) RNA granules living a post-transcriptional life: the trypanosomes' case. *Curr Chem Biol* **5:** 108–117.

Cassola, A., and Frasch, A.C. (2009) An RNA recognition motif mediates the nucleocytoplasmic transport of a trypanosome RNA-binding protein. *J Biol Chem* **284:** 35015–35028.

Cassola, A., De Gaudenzi, J.G., and Frasch, A.C. (2007) Recruitment of mRNAs to cytoplasmic ribonucleoprotein granules in trypanosomes. *Mol Microbiol* **65:** 655–670.

Cassola, A., Noe, G., and Frasch, A.C. (2010) RNA recognition motifs involved in nuclear import of RNA-binding proteins. *RNA Biol* **7:** 339–344.

Cevallos, A.M., Perez-Escobar, M., Espinosa, N., Herrera, J., Lopez-Villasenor, I., and Hernandez, R. (2005) The stabilization of housekeeping transcripts in *Trypanosoma cruzi* epimastigotes evidences a global regulation of RNA decay during stationary phase. *FEMS Microbiol Lett* **246:** 259–264.

Chung, J., Rocha, A.A., Tonelli, R.R., Castilho, B.A., and Schenkman, S. (2013) Eukaryotic initiation factor 5A dephosphorylation is required for translational arrest in stationary phase cells. *Biochem J* **451:** 257–267.

Clayton, C. (2013) The regulation of trypanosome gene expression by RNA-binding proteins. *PLoS Pathog* **9:** e1003680.

Cléry, A., and Allain, F.H.T. (2012) A structural biology perspective of proteins involved in splicing regulation. In *Alternative Pre-mRNA Splicing.* Weinheim, Germany: Wiley-VCH Verlag GmbH & Co. KGaA, pp. 33–48.

Clery, A., Blatter, M., and Allain, F.H. (2008) RNA recognition motifs: boring? Not quite. *Curr Opin Struct Biol* **18:** 290–298.

Cristodero, M., Schimanski, B., Heller, M., and Roditi, I. (2014) Functional characterization of the trypanosome translational repressor SCD6. *Biochem J* **457:** 57–67.

Daubner, G.M., Clery, A., and Allain, F.H. (2013) RRM-RNA recognition: NMR or crystallography . . . and new findings. *Curr Opin Struct Biol* **23:** 100–108.

De Gaudenzi, J., Frasch, A.C., and Clayton, C. (2005) RNA-binding domain proteins in Kinetoplastids: a comparative analysis. *Eukaryot Cell* **4:** 2106–2114.

De Gaudenzi, J.G., D'Orso, I., and Frasch, A.C. (2003) RNA recognition motif-type RNA-binding proteins in *Trypanosoma cruzi* form a family involved in the interaction with specific transcripts in vivo. *J Biol Chem* **278:** 18884–18894.

Deb, T.B., and Datta, K. (1996) Molecular cloning of human fibroblast hyaluronic acid-binding protein confirms its identity with P-32, a protein co-purified with splicing factor SF2. Hyaluronic acid-binding protein as P-32 protein, co-purified with splicing factor SF2. *J Biol Chem* **271:** 2206–2212.

Dedio, J., Jahnen-Dechent, W., Bachmann, M., and Muller-Esterl, W. (1998) The multiligand-binding protein gC1qR, putative C1q receptor, is a mitochondrial protein. *J Immunol* **160:** 3534–3542.

D'Orso, I., and Frasch, A.C. (2001) TcUBP-1, a developmentally regulated U-rich RNA-binding protein involved in selective mRNA destabilization in trypanosomes. *J Biol Chem* **276:** 34801–34809.

D'Orso, I., and Frasch, A.C. (2002) TcUBP-1, an mRNA destabilizing factor from trypanosomes, homodimerizes and interacts with novel AU-rich element- and Poly(A)-binding proteins forming a ribonucleoprotein complex. *J Biol Chem* **277:** 50520–50528.

Droll, D., Minia, I., Fadda, A., Singh, A., Stewart, M., Queiroz, R., and Clayton, C. (2013) Post-transcriptional regulation of the trypanosome heat shock response by a zinc finger protein. *PLoS Pathog* **9:** e1003286.

Fernández-Moya, S.M., and Estévez, A.M. (2010) Posttranscriptional control and the role of RNA-binding proteins in

gene regulation in trypanosomatid protozoan parasites. *Wiley Interdiscip Rev RNA* **1:** 34–46.
Fernandez-Moya, S.M., Carrington, M., and Estevez, A.M. (2014) A short RNA stem-loop is necessary and sufficient for repression of gene expression during early logarithmic phase in trypanosomes. *Nucleic Acids Res* **42:** 7201–7209.
Ghebrehiwet, B., Lim, B.L., Peerschke, E.I., Willis, A.C., and Reid, K.B. (1994) Isolation, cDNA cloning, and overexpression of a 33 kD cell surface glycoprotein that binds to the globular 'heads' of C1q. *J Exp Med* **179:** 1809–1821.
Ghebrehiwet, B., Ji, Y., Valentino, A., Pednekar, L., Ramadass, M., Habiel, D., *et al.* (2014) Soluble gC1qR is an autocrine signal that induces B1R expression on endothelial cells. *J Immunol* **192:** 377–384.
Gingrich, J.C., Davis, D.R., and Nguyen, Q. (2000) Multiplex detection and quantitation of proteins on western blots using fluorescent probes. *Biotechniques* **29:** 636–642.
Han, T.W., Kato, M., Xie, S., Wu, L.C., Mirzaei, H., Pei, J., *et al.* (2012) Cell-free formation of RNA granules: bound RNAs identify features and components of cellular assemblies. *Cell* **149:** 768–779.
Hayman, M.L., Miller, M.M., Chandler, D.M., Goulah, C.C., and Read, L.K. (2001) The trypanosome homolog of human p32 interacts with RBP16 and stimulates its gRNA binding activity. *Nucleic Acids Res* **29:** 5216–5225.
Heyd, F., Carmo-Fonseca, M., and Moroy, T. (2008) Differential isoform expression and interaction with the P32 regulatory protein controls the subcellular localization of the splicing factor U2AF26. *J Biol Chem* **283:** 19636–19645.
Jiang, J., Zhang, Y., Krainer, A.R., and Xu, R.M. (1999) Crystal structure of human p32, a doughnut-shaped acidic mitochondrial matrix protein. *Proc Natl Acad Sci USA* **96:** 3572–3577.
Kato, M., Han, T.W., Xie, S., Shi, K., Du, X., Wu, L.C., *et al.* (2012) Cell-free formation of RNA granules: low complexity sequence domains form dynamic fibers within hydrogels. *Cell* **149:** 753–767.
Kolev, N.G., Ullu, E., and Tschudi, C. (2014) The emerging role of RNA-binding proteins in the life cycle of *Trypanosoma brucei*. *Cell Microbiol* **16:** 482–489.
Kovarova, J., Horakova, E., Changmai, P., Vancova, M., and Lukes, J. (2014) Mitochondrial and nucleolar localization of cysteine desulfurase Nfs and the scaffold protein Isu in *Trypanosoma brucei*. *Eukaryot Cell* **13:** 353–362.
Krainer, A.R., Mayeda, A., Kozak, D., and Binns, G. (1991) Functional expression of cloned human splicing factor SF2: homology to RNA-binding proteins, U1 70K, and Drosophila splicing regulators. *Cell* **66:** 383–394.
Kramer, S. (2014) RNA in development: how ribonucleoprotein granules regulate the life cycles of pathogenic protozoa. *Wiley Interdiscip Rev RNA* **5:** 263–284.
Kumar, G.R., Shum, L., and Glaunsinger, B.A. (2011) Importin alpha-mediated nuclear import of cytoplasmic poly(A) binding protein occurs as a direct consequence of cytoplasmic mRNA depletion. *Mol Cell Biol* **31:** 3113–3125.
Lee, S.R., and Lykke-Andersen, J. (2013) Emerging roles for ribonucleoprotein modification and remodeling in controlling RNA fate. *Trends Cell Biol* **23:** 504–510.
Li, Y.R., King, O.D., Shorter, J., and Gitler, A.D. (2013) Stress granules as crucibles of ALS pathogenesis. *J Cell Biol* **201:** 361–372.
Lunde, B.M., Moore, C., and Varani, G. (2007) RNA-binding proteins: modular design for efficient function. *Nature reviews* **8:** 479–490.
McCall, L.I., and McKerrow, J.H. (2014) Determinants of disease phenotype in trypanosomatid parasites. *Trends Parasitol* **30:** 342–349.
Majumdar, M., Meenakshi, J., Goswami, S.K., and Datta, K. (2002) Hyaluronan binding protein 1 (HABP1)/C1QBP/p32 is an endogenous substrate for MAP kinase and is translocated to the nucleus upon mitogenic stimulation. *Biochem Biophys Res Commun* **291:** 829–837.
Matthews, D.A., and Russell, W.C. (1998) Adenovirus core protein V interacts with p32 – a protein which is associated with both the mitochondria and the nucleus. *J Gen Virol* **79** (Part 7): 1677–1685.
Miller, M.M., and Read, L.K. (2003) *Trypanosoma brucei*: functions of RBP16 cold shock and RGG domains in macromolecular interactions. *Exp Parasitol* **105:** 140–148.
Moore, M.J. (2005) From birth to death: the complex lives of eukaryotic mRNAs. *Science (New York, NY)* **309:** 1514–1518.
Moretti, N.S., and Schenkman, S. (2013) Chromatin modifications in trypanosomes due to stress. *Cell Microbiol* **15:** 709–717.
Muta, T., Kang, D., Kitajima, S., Fujiwara, T., and Hamasaki, N. (1997) p32 protein, a splicing factor 2-associated protein, is localized in mitochondrial matrix and is functionally important in maintaining oxidative phosphorylation. *J Biol Chem* **272:** 24363–24370.
Nett, I.R., Martin, D.M., Miranda-Saavedra, D., Lamont, D., Barber, J.D., Mehlert, A., and Ferguson, M.A. (2009) The phosphoproteome of bloodstream form *Trypanosoma brucei*, causative agent of African sleeping sickness. *Mol Cell Proteomics* **8:** 1527–1538.
Niranjanakumari, S., Lasda, E., Brazas, R., and Garcia-Blanco, M.A. (2002) Reversible cross-linking combined with immunoprecipitation to study RNA-protein interactions in vivo. *Methods* **26:** 182–190.
Noe, G., De Gaudenzi, J.G., and Frasch, A.C. (2008) Functionally related transcripts have common RNA motifs for specific RNA-binding proteins in trypanosomes. *BMC Mol Biol* **9:** 107.
Ouna, B.A., Stewart, M., Helbig, C., and Clayton, C. (2012) The *Trypanosoma brucei* CCCH zinc finger proteins ZC3H12 and ZC3H13. *Mol Biochem Parasitol* **183:** 184–188.
Pereira, M.M., Malvezzi, A.M., Nascimento, L.M., Lima, T.D., Alves, V.S., Palma, M.L., *et al.* (2013) The eIF4E subunits of two distinct trypanosomatid eIF4F complexes are subjected to differential post-translational modifications associated to distinct growth phases in culture. *Mol Biochem Parasitol* **190:** 82–86.
Petersen-Mahrt, S.K., Estmer, C., Ohrmalm, C., Matthews, D.A., Russell, W.C., and Akusjarvi, G. (1999) The splicing factor-associated protein, p32, regulates RNA splicing by inhibiting ASF/SF2 RNA binding and phosphorylation. *EMBO J* **18:** 1014–1024.
Ramaswami, M., Taylor, J.P., and Parker, R. (2013) Altered ribostasis: RNA-protein granules in degenerative disorders. *Cell* **154:** 727–736.

Sahoo, P.K., Murawala, P., Sawale, P.T., Sahoo, M.R., Tripathi, M.M., Gaikwad, S.R., *et al.* (2012) Wnt signalling antagonizes stress granule assembly through a Dishevelled-dependent mechanism. *Biology Open* **1:** 109–119.

Schneider, A., Bursac, D., and Lithgow, T. (2008) The direct route: a simplified pathway for protein import into the mitochondrion of trypanosomes. *Trends Cell Biol* **18:** 12–18.

Singh, A., Minia, I., Droll, D., Fadda, A., Clayton, C., and Erben, E. (2014) Trypanosome MKT1 and the RNA-binding protein ZC3H11: interactions and potential roles in post-transcriptional regulatory networks. *Nucleic Acids Res* **42:** 4652–4668.

Sprehe, M., Fisk, J.C., McEvoy, S.M., Read, L.K., and Schumacher, M.A. (2010) Structure of the *Trypanosoma brucei* p22 protein, a cytochrome oxidase subunit II-specific RNA-editing accessory factor. *J Biol Chem* **285:** 18899–18908.

Stefl, R., Skrisovska, L., and Allain, F.H. (2005) RNA sequence- and shape-dependent recognition by proteins in the ribonucleoprotein particle. *EMBO Rep* **6:** 33–38.

Taylor, M.C., and Kelly, J.M. (2006) pTcINDEX: a stable tetracycline-regulated expression vector for *Trypanosoma cruzi*. *BMC Biotechnol* **6:** 32.

Urbaniak, M.D., Martin, D.M., and Ferguson, M.A. (2013) Global quantitative SILAC phosphoproteomics reveals differential phosphorylation is widespread between the procyclic and bloodstream form lifecycle stages of *Trypanosoma brucei*. *J Proteome Res* **12:** 2233–2244.

Vassella, E., Straesser, K., and Boshart, M. (1997) A mitochondrion-specific dye for multicolour fluorescent imaging of *Trypanosoma brucei*. *Mol Biochem Parasitol* **90:** 381–385.

Volpon, L., D'Orso, I., Young, C.R., Frasch, A.C., and Gehring, K. (2005) NMR structural study of TcUBP1, a single RRM domain protein from *Trypanosoma cruzi*: contribution of a beta hairpin to RNA binding. *Biochemistry* **44:** 3708–3717.

Yagi, M., Uchiumi, T., Takazaki, S., Okuno, B., Nomura, M., Yoshida, S., *et al.* (2012) p32/gC1qR is indispensable for fetal development and mitochondrial translation: importance of its RNA-binding ability. *Nucleic Acids Res* **40:** 9717–9737.

Zhang, X., Zhang, F., Guo, L., Wang, Y., Zhang, P., Wang, R., *et al.* (2013) Interactome analysis reveals that C1QBP (complement component 1, q subcomponent binding protein) is associated with cancer cell chemotaxis and metastasis. *Mol Cell Proteomics* **12:** 3199–3209.

Supporting information

Additional supporting information may be found in the online version of this article at the publisher's web-site.